Lattice dynamics of GaSe

S. Jandl* and J. L. Brebner
Département de Physique, Université de Montréal, Montréal, Québec, Canada

B. M. Powell
Atomic Energy of Canada Ltd., Chalk River, Ontario, Canada

(Received 20 May 1975)

Neutron inelastic scattering measurements of the phonon dispersion relation of GaSe have been analysed in terms of a simple axially symmetric Born–von Kármán force-constant model. The results show that the interlayer interaction is very weak compared with the intralayer ones. The model obtained from this analysis has provided the basis for a calculation of the frequency distribution function for GaSe and this in turn has been used to calculate the Debye temperature and the lattice specific heat as a function of temperature. The agreement with the measured heat capacity is excellent. The two-phonon spectra are also calculated.

I. INTRODUCTION

In recent years there has been considerable interest in the properties of layer structures particularly in the extent to which their two-dimensional nature influences these properties. Dolling and Brockhouse[1] made the first inelastic-neutron-scattering measurements on a layer structure, in this instance, graphite. More recently, pyrolytic graphite has been extensively investigated by Nicklow *et al.*[2] Preliminary results have also been published for $NbSe_2$, MoS_2,[3] and ϵ-GaSe.[4] In the present paper we report further measurements of the phonon dispersion curves in ϵ-GaSe.

In GaSe, the tightly bound layers consist of four two-dimensional sheets of like atoms. Along the major symmetry axis these sheets are in the sequence Se-Ga-Ga-Se, and the strong bonding both within and between the sheets of a particular layer (intralayer forces) is thought to be covalent in character. The complete fourfold layers are bound together by much weaker forces (interlayer), usually considered to be of Van der Waals type. The large difference in the relative strength of the intra- and interlayer forces leads to the pseudo-two-dimensional character of GaSe.

Because the interlayer forces are weak, GaSe may occur in three different polytypes.[4,5] The present specimen was examined by both neutron and Raman scattering and found to be predominantly ϵ polytype. The force system used to interpret the present measurements contains no interaction to second-neighbor layers, and so throughout the present paper we shall consider the crystal as a pure ϵ polytype. The crystal is thus assumed to have an hexagonal structure with space group D^1_{3h}. The unit cell and the Brillouin zone with the group theoretical designation of the major directions and symmetry points are shown in Figs. 1 and 2.

In the present paper, details of the experimental measurements and the general features of the results are discussed in Sec. II, while in Sec. III the results are analyzed in terms of an axially symmetric lattice-dynamical model. The parameters of this model are used to calculate thermodynamical properties in Sec. IV and a brief summary is given in Sec. V.

II. EXPERIMENTAL RESULTS

The single crystal of GaSe used in the present experiments was grown by the Bridgman technique

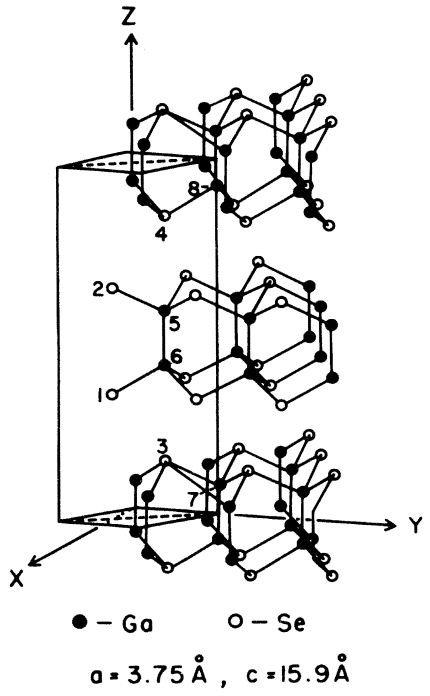

FIG. 1. Unit cell of ϵ-GaSe showing intralayer bonding. The numbered atoms (1–8) are contained in the unit cell.

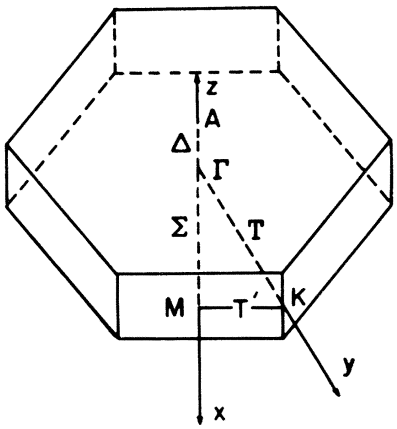

FIG. 2. Brillouin zone.

and was in the form of an ingot ~2.5 cm long. The specimen was oriented with the $[1\bar{2}0]$ direction vertical and the frequencies of phonons propagating along the Δ, Σ symmetry directions of the Brillouin zone were measured by the technique of inelastic neutron scattering. All measurements were made on triple-axis spectrometers operated in their constant momentum transfer mode[6] at a temperature of 100 K. Phonons propagating along the Δ direction were measured at NRU reactor Chalk River. Monochromator and analyzer were Ge (220) and Ge (111) reflections, respectively, and the analyzing energy was fixed at 4.85 THz throughout the series of measurements. Phonons propagating along the Σ direction were measured on the High Flux Isotope Reactor at Oak Ridge. Both monochromator and analyzer were Be (101) reflections, and the incident neutron energy was kept fixed; two values, 8.41 and 6.43 THz, were used. The agreement between the frequency of the same phonons measured on the two spectrometers was excellent. The assignment of the mode responsible for a particular peak in the scattered neutron distribution was made by calculating the one phonon inelastic structure factors on the basis of our proposed dynamical model. The typical experimental error for the frequencies is ~4%. The experimental dispersion curves derived from the comparison of the calculated structure factors and the observed intensities are shown by the symbols in Fig. 3.

The group theoretical labeling is that derived by Jandl and Brebner.[5] In the Σ direction only modes of the Σ_1, Σ_3 symmetry representations are observed; those of the Σ_2, Σ_4 representations have structure factors which are identically zero throughout the scattering plane utilized in the experiments. In the Δ direction the four lowest energy branches represent almost pure rigid-layer modes. They were previously analyzed by Brebner *et al.*[4] to give information about the range of the interlayer forces. The higher-energy branches are calculated to be almost dispersionless and represent predominantly intralayer modes. In the Σ direction this separation into inter- and intralayer modes is less pronounced, and almost all branches show some dispersion. Both Raman[7-13] and infrared[14] measurements have been made on GaSe but there is disagreement over the interpretation of some of these optical measurements.[5] The frequencies of $|\zeta| = 0$ modes measured by the present neutron-scattering results agree well with those determined optically. Ultrasonic measurements of the elastic constants have been made by Khalilov and Rzaev.[15] The velocity of sound lines determined from their results are shown in Fig.

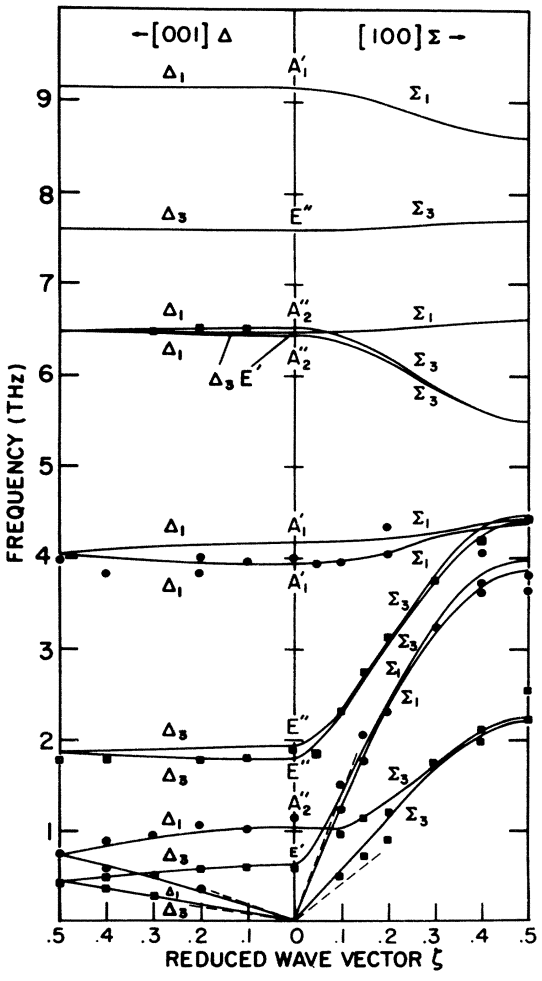

FIG. 3. Comparison of the experimental (symbols) and fitted (solid lines) dispersion curves for the Δ and Σ directions in ϵ-GaSe. Solid circle, Δ_1, Σ_1; solid square, Δ_3, Σ_3.

3 by the dashed lines through the origin for the Δ, Σ directions.

III. ANALYSIS OF RESULTS

The experimental dispersion curves shown in Fig. 3 have been analyzed in terms of an axially symmetric (AS) lattice-dynamical model including only short-range forces. Such a model assumes that the forces between any pair of atoms may be described in terms of a pair potential $V(r)$ depending only on the interatomic separation. The interatomic force constants $\phi_{\alpha\beta}(lk, l'k')$ between atoms (lk), $(l'k')$ can be written[16]

$$\phi_{\alpha\beta}(lk, l'k') = \frac{\epsilon_\alpha \epsilon_\beta}{|\epsilon|^2}(A - B) + \delta_{\alpha\beta} B ,$$

where

$$A \equiv \left(\frac{\partial^2 V(r)}{\partial r^2}\right)_{r=r_0}, \quad B = \left(\frac{1}{r}\frac{\partial V}{\partial r}\right)_{r=r_0},$$

and $\vec{\epsilon} = \vec{r}(l') - \vec{r}(l) + \vec{r}(k') - \vec{r}(k)$, with the derivatives A and B being the independent parameters. We have included the five shortest bonds in the crystal in the force system, and these are specified in Table I. Only one of these bonds, the Se-Se bond, describes an interlayer interaction, the remainder are intralayer interactions. The Ga-Ga bond (No. 4) has an interatomic separation equal to that of the Se-Se bond connecting the Se atoms designated as (1) in adjacent unit cells. Consequently we might include both interactions in the model. However, since the bonds are parallel as well as equal in length, their parameters (A, B) tend to be correlated in fitting to the present experimental frequencies, and we have chosen to specifically include only the Ga-Ga bond in the model. The ten parameters of the model are not independent, for in equilibrium the forces on each atom must sum to zero. If we assume the AS forces are the only ones present in the solid this equilibrium condition leads to the relations

$$3.582B_2 - 9.552B_3 + 10.746B_5 = 0 ,$$

$$2.388B_1 - 3.582B_2 + 10.746B_5 = 0 .$$

A further relation among the force constants is provided by the symmetry requirement that the slopes of the acoustic Δ_3, Σ_3 modes as $|\zeta| \to 0$ are both determined by the elastic constant C_{44}. This condition leads to the relation

$$-2.85B_1 + 2.75B_2 + 0.022A_3 - 11.71B_3$$
$$+21.125B_4 + 0.012A_5 - 31.48B_5 = 0 .$$

From preliminary model fitting it became evident that the terms in A_3, A_5 made rather small contributions to the total expression and they were neglected. The resulting expression was used to define the parameter B_5. Since forces other than AS forces exist in the crystal, we chose not to impose the equilibrium conditions on this simple model. The model then has nine independent parameters. These were determined by "least-squares" fitting to the experimental frequencies, and the dispersion curves calculated from the "best-fit" parameters are compared with experiment in Fig. 3.

TABLE I. Characteristics of the bonds included in the AS model (see Fig. 1).

Bond	Location	Typical pair	r (Å)
Ga-Ga (1)	same layer	(5, 6)	2.388
Ga-Se (2)	same layer	(1, 6)	2.473
Se-Se (3)	two adjacent layers	(1, 3)	3.850
Ga-Ga (4)	same layer, different unit cells	(6, 6)	3.750
Ga-Se (5)	same layer	(1, 5)	4.186

The model evidently provides a fair (quality of fit $\chi = 3.2$) description of the lower-frequency dispersion curves and the higher frequency optical modes. The best-fit parameters are given in Table II. It is evident from the magnitude of the parameters that the Ga-Ga, Ga-Se bonds (1, 2, respectively, of Table I) are significantly stronger than any other bonds of the model, even the additional intralayer bonds 4, 5. The interlayer Se-Se bond is much weaker than the dominant bonds, and their relative magnitudes support the contention of covalent intralayer and Van der Waals interlayer forces.

The calculated dispersion curves along Δ are seen to be generally flat showing little variation with ζ. Along Σ however, most of the branches show significant dispersion. The interlayer interaction is determined primarily from the four lowest-frequency dispersion curves along Δ. The model then predicts the splitting of the conjugate

TABLE II. Force constants for GaSe ($N\,m^{-1}$). (B_5 is determined from the condition required by equality of the slopes of the acoustic Δ_3, Σ_3 branches.)

$A_1 = 131 \pm 7$	$B_1 = 43 \pm 5$
$A_2 = 66 \pm 2$	$B_2 = 19 \pm 1$
$A_3 = 2.5 \pm 0.3$	$B_3 = 0.3 \pm 0.1$
$A_4 = 14 \pm 1$	$B_4 = -3.7 \pm 0.4$
$A_5 = 7 \pm 1$	$B_5 = -5$

modes[4] to be 0.15 THz (5 cm^{-1}) and 0.24 THz (8 cm^{-1}) for the lowest E'' and A_1' modes, respectively. It also predicts the splittings to be smaller for the higher-frequency optical modes. Some splitting measurements have been reported by Hayek *et al.*[10] They observed the splitting for the lowest A_1' mode (0.18 THz) but did not observe any splitting for the lowest E'' mode. Splittings at higher energies have also been reported.

The fitted dispersion curves agree well with the velocity of sound lines derived from the elastic-constant measurements[15] and also generally agree with the optical measurements[7-14] at $|\zeta| = 0$. The optical mode whose frequency is 7.5 THz is predicted to be of E'' symmetry representation while the mode with frequency 6.4 THz is predicted to have E' symmetry. These assignments agree with the group-theory analysis given previously.[5] The most serious discrepancy between the present model and optical measurement is in the frequency of the upper A_2'' mode. The model calculates this mode to have a frequency of 6.5 THz, while the ir measurement[14] indicates a frequency of 7.11 THz. An ir measurement with $\vec{E} \| \vec{c}$, as required for observation of this A_2'' mode, is a difficult one to make reliably in layer compounds such as GaSe. Surface effects for this experimental orientation can easily lead to erroneous results. Consequently, perhaps the difference between the calculated and experimental frequencies for the A_2'' mode is not very significant.

IV. CALCULATIONS

The best-fit parameters have been used to calculate the dispersion curves for the T, T' directions, and these are shown, together with those for Δ, Σ for completeness in Fig. 4. The phonon frequency distribution function $g(\nu)$ was calculated using the method of Raubenheimer and Gilat[17] and the result is shown in Fig. 5. The distribution shows four distinct bands whose origin can be seen from Fig. 4. The lower band arises, at least for the Σ, T, T' directions, from the acoustic and lowest optical modes. This is separated by a frequency gap (~0.8 THz) from the next band of optical modes whose bandwidth is ~1.2 THz. The third band is rather narrow (bandwidth ~0.7 THz) and is separated by a small gap (~0.3 THz) from the second band while the gap between the third and fourth band is ~0.8 THz. The correlation between the dispersion curves shown in Fig. 4 and $g(\nu)$ indicates that the separation of the

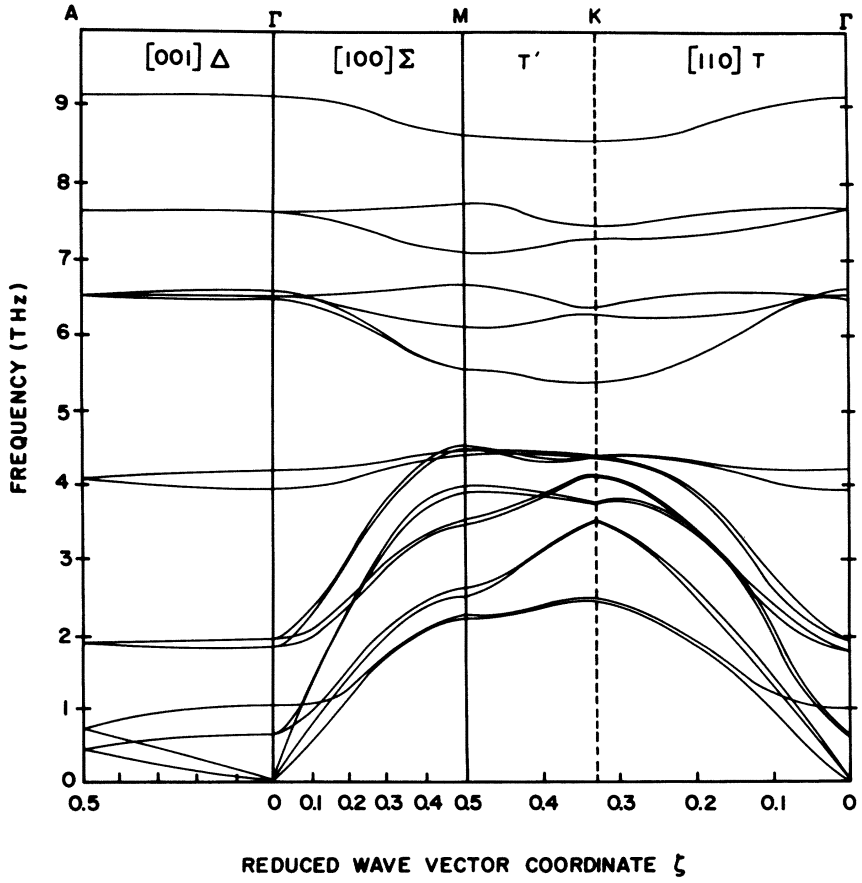

FIG. 4. Calculated dispersion curves for Δ, Σ, T, T' directions.

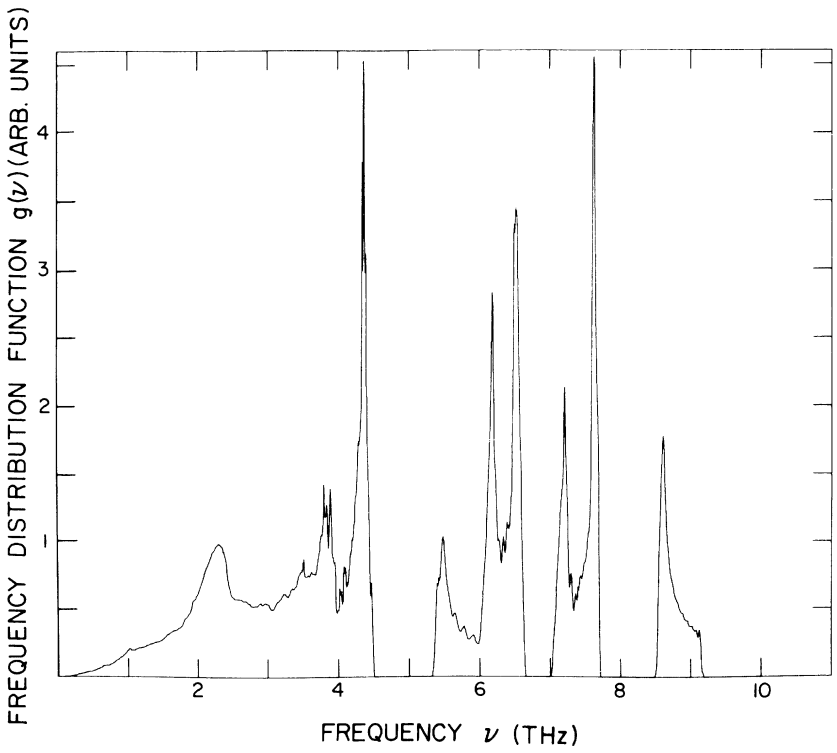

FIG. 5. Phonon frequency distribution function $g(\nu)$.

curves into four well-defined bands also holds for other directions in the Brillouin zone. Several of the prominent critical points in $g(\nu)$ can be correlated with particular modes at Γ. These critical points will have a significant contribution from modes involving simple relative motion of the Ga and Se sublattices. In general, however, the features of $g(\nu)$ cannot be interpreted in terms of such simple modes.

When the distribution function $g(\nu)$ is known, then the lattice specific heat $C_v(T)$ may be calculated. We have computed this quantity from the $g(\nu)$ shown in Fig. 5 assuming that $g(\nu)$ is independent of temperature. The result is shown as the solid line in Fig. 6(a). The solid points show the experimental C_v measured by Mamedov *et al.*[18] The agreement between the present calculation and the observed C_v is excellent. At low temperatures, $C_v \propto T^3$ for normal three-dimensional solids. For pseudo two-dimensional solids, however, there is a temperature range in which $C_v \propto T^2$ and it is of interest to see if this temperature dependence is evident in GaSe. Figure 6(b) shows a plot of C_v vs T on a log-log scale. For low temperatures (<16 K), the curve is a straight line with a gradient 2.8 ± 0.1, thus in this temperature range C_v has, approximately, the characteristic T^3 behavior. For temperatures between 16 and 30 K, however, the curve is a different straight line, whose gradient is 2.1 ± 0.1. Consequently, in this temperature range, GaSe seems to show behavior which is very close to that of a pure two-dimensional solid.

At any given temperature the specific heat C_v, calculated "exactly" from the distribution function $g(\nu)$, may be equated to the corresponding quantity calculated on the basis of a Debye model. In this manner an effective Debye temperature Θ_D may be determined for any temperature. The temperature variation of the Debye temperature of GaSe is shown in Fig. 7. The curve does not show the minimum which is characteristic of this function for many solids. As $T \to 0$, $\Theta_D = 187$ K and then steadily increases to a high-temperature value ($T \to \infty$), $\Theta_D = 342$ K.

In addition to the one-phonon scattering processes which have been utilized to determine the phonon dispersion curves, there may also be scattering processes involving two phonons. The energy transfer in such a scattering process is given by

$$h\nu = h\nu_j(\vec{q}) \pm h\nu_{j'}(\vec{q}') ,$$

while the wave-vector transfer is given by

$$\vec{Q} = \vec{\tau} + \vec{q} + \vec{q}' .$$

For optical scattering methods $\vec{Q} \approx \vec{\tau} = 0$, i.e., $\vec{q} = -\vec{q}'$. The detailed theory of two-phonon scattering involves selection rules specifying which pair of modes may scatter the probe. However, the intensity of two-phonon scattering will depend, among other things, on the two-phonon density of states. We have calculated the two-phonon distribution functions from the function $g(\nu)$ in Fig. 5. The overtone distribution $g(2\nu)$ is identical to that of Fig. 5 with the frequency scale doubled. The combination (sum and difference) spectra are calculated by adding or subtracting the frequencies of phonons having the same wave vector from different branches. No selection rules have been applied. The results for the sum, $g(\nu + \nu')$ and difference $g(\nu - \nu')$ spectra are shown in Figs. 8(a) and 8(b). Both spectra show a great deal of structure as would be expected from the highly structured nature of the one-phonon distribution function $g(\nu)$.

A large number of frequencies were observed in the two-phonon Raman spectrum of GaSe by Yoshida *et al.*[11] These authors interpreted their spectrum in terms of combinations of phonons at Γ. However, we can see that the structures of the overtone, sum and difference spectra allow much more flexibility in the assignment of the observed peaks. All the peaks observed by Yoshida *et al.* can be assigned to features in one or other of the two-phonon spectra, with the exception of the highest-energy observed peak at 18.0 THz. We cannot satisfactorily interpret this peak in terms of any two-phonon combination.

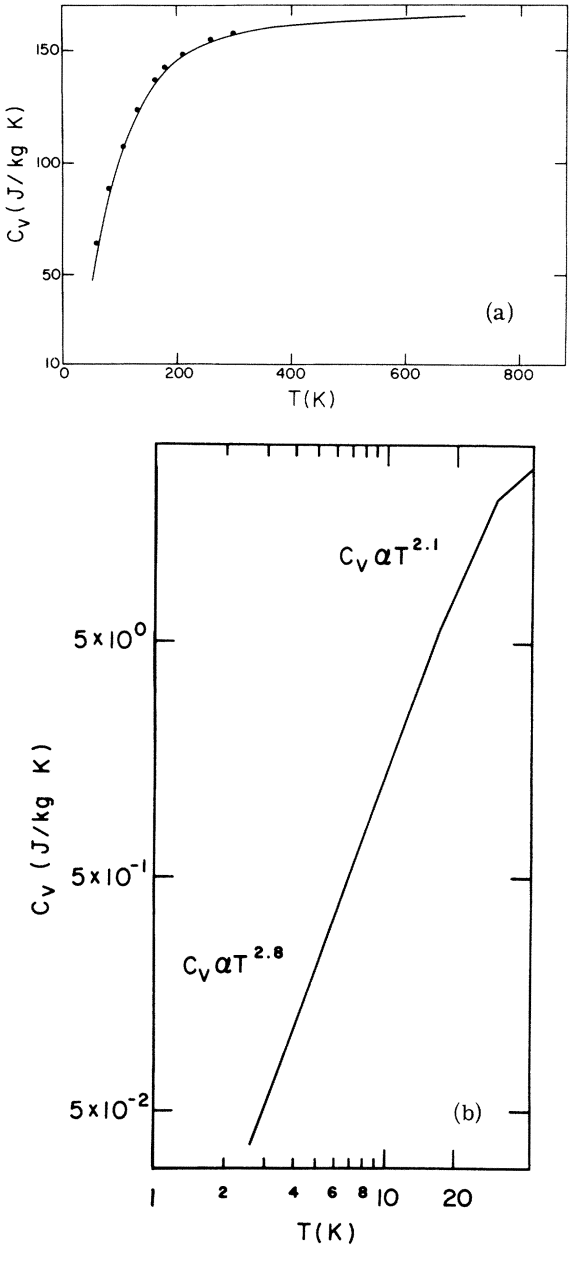

FIG. 6. (a) Temperature dependence of the specific heat $C_v(T)$ calculated from $g(\nu)$. The result of the calculation is shown as the solid line and the solid points represent the experimental measurements of Mamedov (Ref. 18). (b) Log-log plot of the temperature dependence of C_v at low temperatures.

V. SUMMARY

Measurements have been made of the acoustic and low-energy optical dispersion curves of modes propagating in the Δ, Σ directions of GaSe at 100 K. In the Δ direction, the lowest four branches represent interlayer modes, i.e., modes in which the fourfold layers move primarily as rigid units. This separation into inter- and intralayer modes is less pronounced in the Σ direction. The neutron

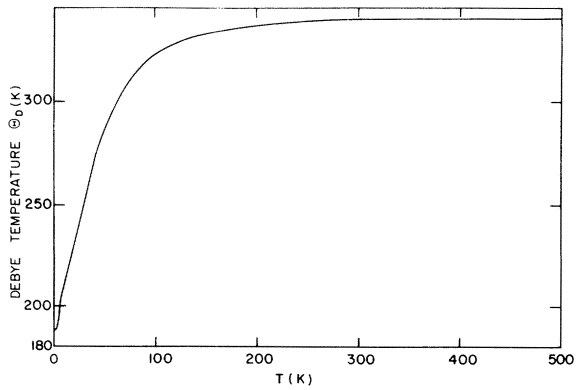

FIG. 7. Temperature dependence of the Debye-temperature $\Theta_D(T)$.

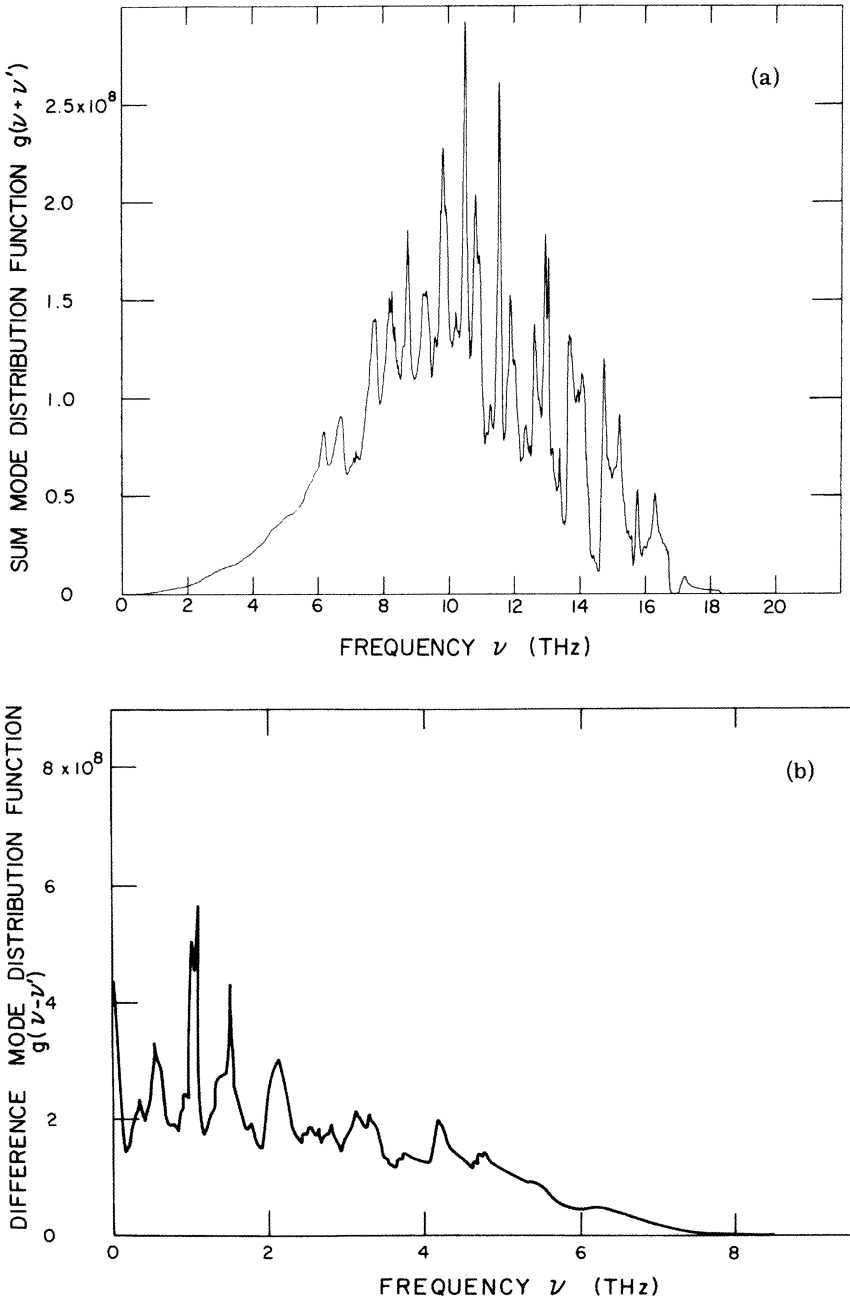

FIG. 8. (a) Two-phonon sum spectrum $g(\nu+\nu')$. (b) Two-phonon difference spectrum $g(\nu-\nu')$.

measurements show fair agreement with optical results and velocity of sound measurements where comparison can be made. The dispersion curves have been analyzed in terms of a simple dynamical model in which the five shortest bonds in the crystal were represented as axially symmetric forces. The model provided a reasonable fit to the experimental results, and the magnitudes of the parameters indicated that the interlayer forces (a Se-Se bond) were significantly weaker (by a factor ~50) than the strongest intralayer forces (a Ga-Ga bond). The temperature dependence of the specific heat calculated from this model showed a region in which $C_v \propto T^{2.1}$, indicating that GaSe behaves as a pseudo-two-dimensional solid at these temperatures.

ACKNOWLEDGMENTS

We are grateful to Dr. H. G. Smith and Dr. R. Nicklow of Oak Ridge National Laboratory for their hospitality and for helpful discussions.

*Present address: Département de Physique, Université de Sherbrooke, Sherbrooke, Québec, J1K 2R1, Canada.

[1]G. Dolling and B. N. Brockhouse, Phys. Rev. 128, 1120 (1962).
[2]R. Nicklow, N. Wakabayashi, and H. G. Smith, Phys. Rev. B 5, 4951 (1972).
[3]N. Wakabayashi, H. G. Smith, and R. M. Nicklow, Phys. Rev. B 12, 659 (1975).
[4]J. L. Brebner, S. Jandl, and B. M. Powell, Solid State Commun. 13, 1555 (1973).
[5]S. Jandl and J. L. Brebner, Can. J. Phys. 52, 2454 (1974).
[6]B. N. Brockhouse, in *Inelastic Scattering of Neutrons in Solids and Liquids* (IAEA, Vienna, 1961), p. 113.
[7]G. B. Wright and A. Mooradian, Bull. Am. Phys. Soc. 11, 812 (1966).
[8]T. J. Wieting and J. L. Verble, Phys. Rev. B 5, 1473 (1972).
[9]J. C. Irwin, R. M. Hoff, B. P. Clayman, and R. A. Bromley, Solid State Commun. 13, 1531 (1973).
[10]M. Hayek, O. Brafman, and R. M. A. Lieth, Phys. Rev. B 8, 2772 (1973).
[11]H. Yoshida, S. Nakashima, and A. Mitsuishi, Phys. Status Solidi B 59, 655 (1973).
[12]A. Mercier and J. P. Voitchovsky, Solid State Commun. 14, 757 (1974).
[13]R. M. Hoff and J. C. Irwin, Phys. Rev. B 10, 3464 (1974).
[14]P. C. Leung, G. Andermann, W. G. Spitzer, and C. A. Mead, J. Phys. Chem. Solids 27, 849 (1966); E. Finkman and A. Rizzo, Solid State Commun. 15, 1841 (1974).
[15]K. M. Khalilov and K. I. Rzaev, Sov. Phys.-Crystallogr. 11, 786 (1957).
[16]G. W. Lehman, T. Wolfram, and R. E. De Wames, Phys. Rev. 128, 1593 (1962).
[17]L. J. Raubenheimer and G. Gilat, Phys. Rev. 157, 586 (1967).
[18]K. K. Mamedov, I. G. Kerimov, V. N. Kostryukov, and M. I. Mekhtiev, Sov. Phys.-Semicond. 1, 363 (1967).